

MID MESOZOIC FLORAS AND CLIMATES

by R. N. L. B. HUBBARD *and* M. C. BOULTER

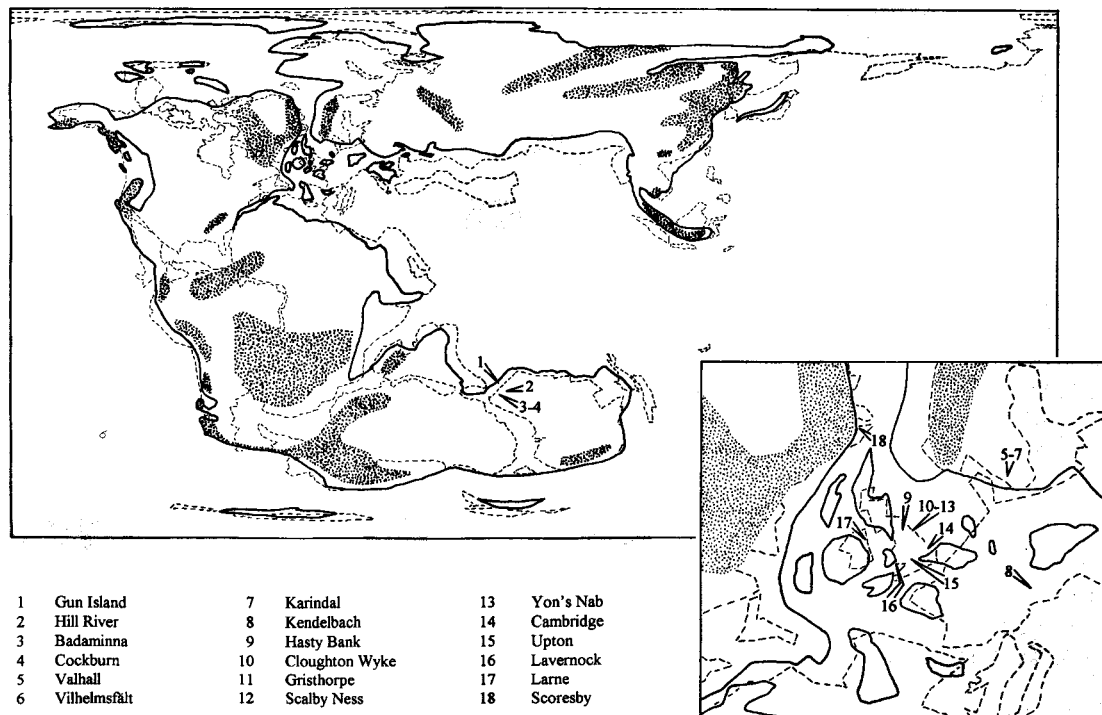
ABSTRACT. Multivariate statistical analyses of pollen and spore assemblages from Late Triassic to Early Cretaceous sedimentary strata in north-west Europe and earlier Jurassic deposits in Western Australia have allowed the identification of three major climatic-ecological groupings in each area. In each hemisphere the sporomorph groupings are interpreted as reflecting semi-tropical, cool-temperate, and intermediate climatic conditions. Only about 8 per cent. of the pollen and spore taxa occur in both hemispheres; among these, there is a high degree of consistency in climatic-ecological behaviour between north and south. When the constituents of the groups are plotted as summary pollen diagrams in the conventional Quaternary palynological manner, climatic 'fingerprints' emerge which allow correlations of hitherto unprecedented accuracy, whether within a region or between hemispheres. The changing proportions of the different groupings allow the first pollen-based quantitative reconstructions of Jurassic climates to be made.

UNIFORMITARIANISM is one of the foundations of geology. We present the results of a decade-long study of Jurassic palynology, in which techniques that were applied successfully to elucidate Cenozoic palynology (Hubbard and Boulter 1983) are applied to Lower and Middle Jurassic pollen (strictly, miospore) analyses. In both cases, multivariate statistical methods were used to find the natural patterns of association in the pollen analyses, and the climatic conditions associated with the various vegetations were deduced. Summary diagrams displaying the interplay of the major vegetational-climatic groupings then allow correlation with the global temperature record which the diagrams reflect. In the Tertiary, pollen diagrams can be correlated with oxygen isotope records and dinoflagellate cyst diagrams (Hubbard *et al.* 1994); in the Jurassic, the oxygen isotope record cannot be used, but correlations between Australia and Europe, and with dinoflagellate cyst diagrams, leave little doubt that global temperature proxies are likewise involved.

Quantitative palynology, in the form of pollen diagrams, is arguably the single most powerful tool of Quaternary palaeoecologists, and is regularly used for correlation and vegetational reconstruction at local to global scales. That palynology is used in analogous ways less and less in earlier geological periods reflects the fact that ecological understanding is almost essential for such treatment. We report here the results of multivariate statistical analyses of Late Triassic to Early Cretaceous pollen assemblages from Australia and Europe. From these analyses we have produced objective syntheses of ecological and climatic developments, and present the first continuous, quantitative reconstructions of Late Triassic and earlier Jurassic palaeoecology and climate. Our pollen diagrams give a global perspective over about 40 million years, for a period the climatic history of which has hitherto been largely speculative.

SOURCES OF DATA

Our study has twin foundations at what are now opposite ends of the globe, but which were considerably closer between 100 and 200 million years ago. Filatoff (1975) has published 246 detailed, high quality palynological analyses from some deep boreholes in Western Australia, which in earlier Jurassic times was at a latitude of about 45° S on the eastern seaboard of the temperate zone of Pangaea (Text-fig. 1). North-west Europe occupied an east-central sub-tropical position (30° N) in the super-continent, about 70° west of Western Australia. In later Jurassic–Early Cretaceous times the development of the precursor of the Atlantic Ocean took place to the south-west, forming a large sub-tropical sea.



TEXT-FIG. 1. Palaeogeographical map showing the Earth in early Jurassic times (Europe and east Greenland enlarged in the inset on the right), and the locations of the critical sections and boreholes discussed in this analysis. Upland areas are stippled, ancient coastlines are shown with a solid line, and modern coastlines (or plate margins) are pecked.

Pollen analytical investigations of Mesozoic strata have been carried out in Europe over four decades by a number of microscopists (Couper 1958; Norris 1963; Muir 1964; Guy 1971; Wilkinson 1978; Guy-Ohlson 1981, 1982, 1990; Riding 1983). The assembling of a 712-taxon master list of pollen and spore types was an essential preliminary stage in the analysis of the European data. From this list, 153 generally recognizable form-genera were isolated (Boulter and Windle 1993). As the analysis proceeded, this definitive classification was reduced by further lumping and synonymy to an irreducible core of 73 Jurassic pollen and spore taxa, upon which our conclusions are based. An additional corpus of related data involved Late Triassic pollen analyses from Europe and Greenland (Orbell 1972, 1973; Morbey 1975; Lund 1977), which at that time were at about 40° N on the north-west corner of Pangaea. These additional Triassic data added a further 36 palynomorph taxa to the master list.

ANALYTICAL METHODS

The analytical methods employed in this study are essentially the same as used earlier to elucidate Tertiary plant ecology (Hubbard and Boulter 1983). The pollen counts were turned into percentages, and these were used to construct a matrix of Pearson's product-moment correlation coefficients, which (in turn) was investigated by principal components and cluster analyses. They are standard techniques of Quaternary palaeoecology (see, for instance, Birks and Birks 1980), and are much the same as those employed by Imbrie and Kipp (1971) in studying the climatic significance of Pleistocene foraminifera, a work that inspired our studies.

Our primary analytical tool was principal components analysis, which defined the associations implied in the correlation matrix. Examination of the co-ordinate plots of the loadings of the (unrotated) principal components, the stratigraphical distributions of the scores of the rotated principal components, and the cluster analyses allowed us to identify three major groups of pollen and spore types in each hemisphere: S I, S II and S III in the southern hemisphere, N I, N II and N III in the northern. Rotated principal components for which samples from different localities score heavily in the same chronological period tend to be related climatically. Taxa sharing climatic-ecological affinities tend to be grouped together in the co-ordinate plots of the unrotated principal components, and in the cluster analyses. By checking the implications of each of these lines of evidence against each other, misattributions can be identified and eliminated. Tables 1 and 2 give the composition of the first four unrotated principal components from the Australian and European data-sets respectively; the figures describe the overall structures inherent in the data. The groupings are indicated in the dendrograms (Text-figs 2–3) which illustrate these relationships; the groupings are derived from the principal components analyses, and the dendrograms are merely a convenient and readily-comprehended way of summarizing the analytical results. It should be remembered that the dendrograms are two-dimensional representations of the complex patterns inherent in the correlation matrices. The simplification involved is one reason why the patterns in the dendrograms often deviate from the mathematically controlled truths of the principal components solutions. The composition of the Australian and European rotated principal components is outlined in Tables 3 and 4.

In the northern hemisphere, the most conspicuous patterns involve groups of tropical spores and pollen that were particularly well represented in later Jurassic and Early Cretaceous times (Group N III, Text-fig. 3); and an opposing group that recorded a dramatic, intense, and extended cold episode around the Triassic–Jurassic (Rhaetian–Hettangian) boundary (Group N I, Text-fig. 3). The southern intermediate group (S II, Text-fig. 2) is particularly well represented in the Australian earlier Jurassic strata, whose conspicuously red colour suggested to Filatoff (1975) that they were deposited in either a tropical or an arid environment. As the representation of the tropical Group S III is trivial, the arid alternative is indicated. This is of considerable relevance to the northern hemisphere results, where the analogous group is common – in some cases (not considered here), almost certainly misleadingly over-represented – in the Late Triassic and earlier Jurassic sequences, but becoming much rarer in the later Jurassic and Early Cretaceous.

The palynological consistency, and steady sediment accumulation rates (attested by the age-*versus*-depth plots) in many of the Australian borehole analyses allow the best sections of their records (Badaminna 1, Gun Island 1, and Cockburn 1) to be overlapped, to give a long and detailed climatic history of the earlier Jurassic (Text-fig. 4), once allowance had been made for identified unconformities and changes in sedimentation rates. Text-figure 5 shows the age-*versus*-depth plots for the three crucial sections: the inconsistencies in the most closely controlled parts are about 100 000 years. Text-figure 4 was compiled using the results from Cockburn 1 from 155 to 166 Ma, Badaminna 1 to 177 Ma, and then Gun Island 1. In the oldest parts of the sequences (earlier than about 184 Ma) the stratigraphical control degrades rapidly. The upper part of the Badaminna 1 sequence (above 650 m) seemed anomalous: the oscillations in the pollen diagram were inconsistent with the records from Filatoff's other sequences covering this period. It was therefore rejected. To preserve integrity, no points were interpolated from another core where the basic shape of the pollen curves would have changed in consequence. The top of the Australian sequences were believed to be approximately Callovian–Oxfordian, while certain central parts were associated with ammonite faunas that linked them with the earliest part of the European Bajocian (Filatoff 1975).

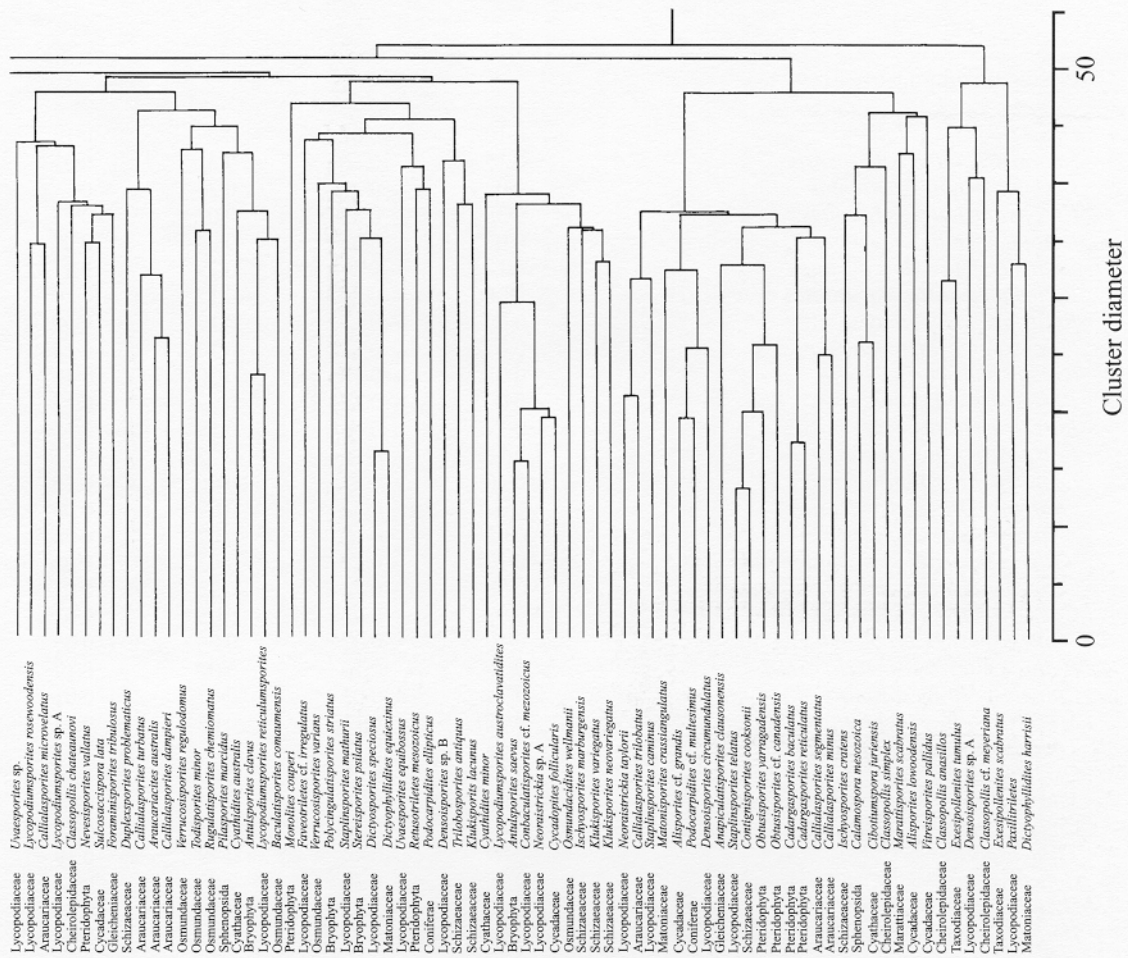
In the palynological dendrograms (Text-figs 2–3) we have attempted to relate pollen and spore types to extinct groups of plants in the hopes of clarifying the 'story' the diagrams tell. This exercise is highly contentious for two reasons: (1) the higher levels of classification in all taxonomic schemes are increasingly abstract intellectual speculations, involving increasing proportions of interpretation; and (2) the relationship between taxonomic structures and pollen and spore morphology is notoriously complicated, and each palynologist dealing with extinct plants will tend to have their

TABLE 1. The first four unrotated principal components yielded by the Australian data. They account for 19.5 per cent. of the variance in the correlation matrix.

Principal component:	1	2	3	4
<i>Stereisporites psilatus</i>	0.32	-0.13	0.01	-0.08
<i>Stereisporites antiquasporites</i>	0.55	-0.03	0.06	-0.16
<i>Rogalskaisporites cicatricosus</i>	0.48	-0.24	0.01	-0.22
<i>Rogalskaisporites canaliculus</i>	0.76	-0.16	0.01	-0.18
<i>Polycingulatisporites crenulatus</i>	0.47	-0.23	-0.01	-0.29
<i>Polycingulatisporites striatus</i>	0.10	-0.08	-0.11	-0.16
<i>Antulsporites varigranulatus</i>	0.39	-0.40	-0.14	-0.13
<i>Antulsporites clavus</i>	0.20	0.09	0	-0.09
<i>Antulsporites saevus</i>	0.29	-0.36	0.51	0.41
<i>Foveosporites moretonensis</i>	0.54	-0.16	-0.12	-0.14
<i>Staplinsporites caminus</i>	0.13	-0.02	-0.14	-0.17
<i>Staplinsporites telatus</i>	0.44	0.50	0.14	-0.01
<i>Staplinsporites mathurii</i>	0.22	-0.04	-0.06	-0.20
<i>Staplinsporites perforatus</i>	0.47	0.18	0.08	-0.04
<i>Foveosporites multifoveolatus</i>	0.37	0.13	0.05	-0.06
<i>Foveotriletes cf. irregulatus</i>	-0.03	-0.12	-0.14	-0.09
<i>Densoisporites circumundulatus</i>	0.09	-0.12	-0.03	-0.10
<i>Densoisporites sp. A</i>	-0.05	0	-0.04	-0.05
<i>Densoisporites sp. B</i>	0.16	-0.31	-0.13	0.01
<i>Lycopodiacidites cerniidites</i>	0.20	-0.21	-0.10	-0.11
<i>Camazonosporites ramosus</i>	0.63	-0.04	0.11	-0.26
<i>Camazonosporites clivus</i>	0.72	0.25	0.17	-0.25
<i>Leptolepidites major</i>	0.30	-0.25	-0.13	-0.06
<i>Uvaesporites equibossus</i>	0.16	-0.29	-0.13	-0.06
<i>Uvaesporites crassibalteus</i>	0.24	-0.27	-0.09	0.03
<i>Uvaesporites sp.</i>	-0.01	0.02	-0.01	0.04
<i>Lophotriletes sp.</i>	0.25	-0.34	-0.17	-0.07
<i>Apiculatosporites</i>	0.43	0.20	0.02	-0.07
<i>Acanthotriletes levindensis</i>	0.22	0.34	-0.38	0.56
<i>Conbaculatisporites cf. mesozoicus</i>	0.04	-0.33	0.56	0.46
<i>Neoraistrickia taylorii</i>	0.12	-0.09	-0.12	-0.08
<i>Neoraistrickia pilobaculata</i>	0.62	0.06	0.09	-0.08
<i>Neoraistrickia trichosa</i>	0.51	0.28	-0.34	0.40
<i>Neoraistrickia densata</i>	0.63	0.14	0.17	-0.22
<i>Neoraistrickia truncata</i>	0.61	0.14	0.05	-0.08
<i>Neoraistrickia sp. A</i>	0.32	-0.37	0.56	0.33
<i>Neoraistrickia spp.</i>	0.54	0.12	-0.28	0.36
<i>Lycopodiumsporites rosewoodensis</i>	-0.17	0	-0.11	-0.08
<i>Lycopodiumsporites reticulumsporites</i>	0.34	-0.13	-0.13	-0.15
<i>Lycopodiumsporites austroclavatis</i>	0.39	0.10	-0.15	0.37
<i>Lycopodiumsporites circolumensis</i>	0.64	0.19	0.11	-0.13
<i>Lycopodiumsporites sp. A</i>	-0.12	0.10	0.01	-0.16
<i>Lycopodiumsporites spp.</i>	0.58	-0.04	0.10	-0.18
<i>Dictyosporites speciosus</i>	0.30	-0.02	0.09	-0.07
<i>Dictyosporites complex</i>	0.41	0.30	-0.37	0.43
<i>Paxillitriletes</i>	-0.11	0.10	0	-0.03
<i>Pilasporites marcidus</i>	-0.16	-0.04	-0.03	-0.02
<i>Calamospora mesozoica</i>	-0.12	0.03	-0.02	-0.09
<i>Marattisporites scabratus</i>	-0.12	-0.07	0.05	0.06
<i>Todisporites minor</i>	-0.16	0.05	0.15	-0.03
<i>Osmundacidites wellmanii</i>	0.20	-0.08	0.47	0.26

TABLE 1. (cont.)

Principal component:	1	2	3	4
<i>Baculatisporites comaumensis</i>	0.13	-0.22	-0.09	-0.07
<i>Verrucosisporites varians</i>	0.10	-0.21	-0.17	-0.08
<i>Verrucosisporites rugulodorus</i>	-0.15	0.04	-0.06	-0.07
<i>Rugulatisporites chamionatus</i>	-0.18	0.10	0.07	-0.16
<i>Cyathidites australis</i>	0.12	0.04	0.07	-0.04
<i>Cyathidites minor</i>	-0.05	-0.15	0.02	0.09
<i>Cibotiumspora juriensis</i>	-0.06	-0.13	-0.09	-0.20
<i>Dictyophyllidites equixinus</i>	0.23	0.02	0.07	0.02
<i>Dictyophyllidites harrisii</i>	-0.23	0.16	0.11	-0.12
<i>Matoniasporites crassiangulatus</i>	-0.12	0.10	0.03	-0.15
<i>Anapiculatisporites clausonensis</i>	-0.05	0.27	0.07	-0.18
<i>Foraminisporites tribulosus</i>	-0.13	0.10	0.04	-0.13
<i>Gleicheniidites senonicus</i>	0.48	0.03	0.15	0.13
<i>Duplexsporites problematicus</i>	-0.03	0.08	-0.53	0.40
<i>Contignisporites cooksonii</i>	0.58	0.54	0.14	-0.03
<i>Trilobosporites antiquus</i>	0.12	-0.12	-0.10	0.05
<i>Ischyosporites cratens</i>	0.05	0.09	-0.09	-0.02
<i>Ischyosporites vollcheimani</i>	0.09	-0.09	-0.03	0.01
<i>Ischyosporites marburgensis</i>	-0.12	0.01	0.04	0.06
<i>Klukisporites variegatus</i>	-0.29	0.11	0.10	-0.05
<i>Klukisporites neovariegatus</i>	0.05	0	0.01	0.02
<i>Klukisporites lacunus</i>	0.02	0.16	-0.11	0.04
<i>Klukisporites scaberis</i>	0.44	-0.11	0	-0.06
<i>Lygodioidisporites perverrucatus</i>	0.16	-0.28	-0.08	0.05
<i>Retusotriletes mesozoicus</i>	-0.03	-0.11	-0.11	0
<i>Granulatisporites</i> sp.	0.02	-0.16	-0.13	-0.01
<i>Convrrucosisporites variverrucatus</i>	0.20	-0.17	-0.10	-0.04
<i>Cadargasporites baculatus</i>	-0.08	0.34	0.29	0.01
<i>Cadargasporites reticulatus</i>	-0.10	0.16	0.27	-0.03
<i>Nevesisporites vallatus</i>	-0.15	0.14	0.11	-0.13
<i>Murospora florida</i>	0.50	0.15	0.14	-0.10
<i>Lycopodiacidites asperatus</i>	0.46	0.32	0.09	0.01
<i>Monolites couperi</i>	-0.06	0	-0.04	-0.03
<i>Reticuloidisporites</i> sp.	0.47	-0.33	-0.05	-0.27
<i>Obtusisporites yarragadensis</i>	0.26	0.41	0.06	0.09
<i>Obtusisporites</i> cf. <i>canadensis</i>	0.18	0.18	-0.01	0.07
<i>Cycadopites follicularis</i>	0.11	-0.27	0.54	0.32
<i>Vitreisporites pallidus</i>	-0.07	-0.05	0.07	0.05
<i>Sulcosaccispora lata</i>	-0.22	0.18	0.06	-0.25
<i>Alisporites lowoodensis</i>	-0.02	-0.08	0.23	0.23
<i>Alisporites</i> cf. <i>grandis</i>	-0.07	0.03	0.11	-0.03
<i>Pinuspollenites parvisaccatus</i>	0.34	-0.04	-0.18	0.27
<i>Pinuspollenites globosaccus</i>	0.24	-0.03	-0.24	0.43
<i>Podocarpidites ellipticus</i>	0.04	0.29	0.04	0.27
<i>Podocarpidites</i> cf. <i>verrucosus</i>	0.11	-0.22	-0.18	0.12
<i>Podocarpidites</i> cf. <i>multesimus</i>	0.27	-0.13	0.07	-0.03
<i>Podosporites castellanosi</i>	0.18	0.17	-0.03	0.31
<i>Araucariacites australis</i>	0.07	-0.08	-0.34	-0.13
<i>Callialasporites segmentatus</i>	-0.16	0.20	0.19	-0.05
<i>Callialasporites minus</i>	-0.07	-0.05	0.48	0.19
<i>Callialasporites microvelatus</i>	-0.12	-0.04	-0.11	-0.17
<i>Callialasporites dampieri</i>	0.09	-0.07	-0.32	0.06
<i>Callialasporites turbatus</i>	-0.27	-0.04	-0.32	0.05



TEXT-FIG. 2. Average Link dendrogram showing the relationships between the 112 Australian Jurassic pollen and spores in the 246 samples involved in this study. Sporomorphs of essentially cold environments (identified from the principal components analyses) are designated as Group S I, thermophilous ones are classified as Group S III; and Group S II contains the climatically intermediate taxa, which are also apparently associated with arid conditions. The family attributions are those of Filatoff (1975).

TABLE 2. The first four unrotated principal components yielded by the European data. They account for 15·7 per cent. of the variance in the correlation matrix.

Principal component:	1	2	3	4
<i>Stereisporites stereoides</i>	0·36	-0·28	-0·08	-0·09
<i>Stereisporites antiquasporites</i>	0·23	-0·14	0·15	0·28
<i>Sculptisporis seeburgensis</i>	-0·04	-0·01	0·04	0·03
<i>Foveasporis irregularis</i>	-0·12	-0·44	0·55	-0·20
<i>Polycingulatisporites circulus</i>	0·45	-0·14	0·06	-0·17
<i>Staplinisporites caminus</i>	-0·15	-0·37	-0·25	-0·09

TABLE 2. (cont.)

Principal component:	1	2	3	4
<i>Densoisporites velatus</i>	-0.10	-0.02	0.27	0.18
<i>Neoraistrickia gristhorpensis</i>	-0.15	-0.16	0.31	0.21
<i>Lycopodiacidites rugulatus</i>	-0.08	-0.21	0.26	0
<i>Lycopodiacidites cerniidites</i>	0.38	-0.23	0.02	-0.13
<i>Lycopodiacidites rhaeticus</i>	0.07	-0.03	0.04	0.07
<i>Retitriletes pseudoreticulatus</i>	0.12	-0.21	0.29	0.47
<i>Retitriletes austroclavatidites</i>	-0.06	-0.34	-0.17	-0.10
<i>Retitriletes clavatoides</i>	-0.09	-0.18	0.12	0.50
<i>Foveotriletes microreticulatus</i>	-0.07	-0.11	0.17	0.14
<i>Lycopodiumsporites</i> sp. A	-0.05	-0.15	0.20	0.48
<i>Rotverrusporites major</i>	-0.09	-0.15	-0.07	-0.13
<i>Rotverrusporites equatibossus</i>	-0.14	-0.46	0.59	-0.16
<i>Rotverrusporites bossus</i>	-0.12	-0.16	0.29	-0.05
<i>Leptolepidites plurituberosus</i>	-0.10	-0.43	-0.06	-0.25
<i>Contignisporites glebulentus</i>	0.07	-0.32	0.07	-0.05
<i>Aequitriradites spinulosus</i>	-0.01	-0.10	-0.07	-0.06
<i>Vallizonosporites pseudoalveolatus</i>	-0.10	-0.17	-0.03	-0.01
<i>Cicatricosisporites brevillaeurae</i>	-0.08	-0.12	-0.22	0.02
<i>Couperisporites complexus</i>	-0.08	-0.02	-0.05	0.02
<i>Duplexisporites problematicus</i>	-0.10	-0.32	0.06	-0.05
<i>Heliosporites reissingeri</i>	0.35	-0.10	0.02	-0.17
<i>Calamospora mesozoica</i>	0.24	-0.05	0.07	0.01
<i>Marattisporites scabratus</i>	0.02	-0.11	0.02	0.32
<i>Todisporites major + minor</i>	-0.64	0.12	0	0.27
<i>Osmundacidites wellmanii</i>	0.23	-0.23	0.09	0.16
<i>Pilosisporites brevipappillosus</i>	-0.05	-0.10	-0.14	0
<i>Concavisporites crassexinus</i>	0.42	-0.12	0.13	0.12
<i>Trilobosporites bernissartensis</i>	-0.09	-0.40	-0.29	-0.19
<i>Concavissimisporites variverrucatus</i>	0.28	-0.38	-0.08	-0.18
<i>Deltoidospora australis</i>	-0.22	-0.02	0.16	0.24
<i>Deltoidospora concavus</i>	-0.04	0	0.25	0.02
<i>Deltoidospora neddeni</i>	0.72	-0.18	0.10	-0.04
<i>Deltoidospora equixinus</i>	-0.13	-0.27	-0.22	0.15
<i>Dictyophyllidites harrisii</i>	-0.16	0	0.13	0.03
<i>Camarozonosporites rudis</i>	0.46	-0.15	0.06	-0.10
<i>Krauselisporites linearis</i>	-0.10	0.06	0.14	-0.07
<i>Endosporites rhysoseus</i>	-0.06	-0.25	-0.17	-0.17
<i>Endosporites jurassicus</i>	-0.11	-0.38	0.49	-0.14
<i>Matonisporites crassiangulatus</i>	-0.05	-0.02	0.01	0.13
<i>Cibotiumspora sinuata</i>	-0.21	-0.06	0.41	-0.04
<i>Cibotiumspora tricuspadata</i>	-0.04	0.02	0.03	-0.03
<i>Obtusisporis canadensis</i>	-0.14	0.08	0.21	-0.15
<i>Gleicheniidites senonicus</i>	-0.13	-0.20	-0.31	0
<i>Ischyosporites lacunus</i>	-0.24	-0.40	0.34	-0.23
<i>Trachysporites asper</i>	0.01	0	0.03	0.10
<i>Undulatisporites concavus</i>	-0.14	-0.33	0.48	0.06
<i>Triancoraesporites ancorae</i>	0.48	0	0.09	-0.07
<i>Platyptera trilingua</i>	-0.04	-0.05	0.08	0.04
<i>Convolutispora microrugulatus</i>	0.49	-0.12	0.07	-0.14
<i>Auritulinasporites scanicus</i>	-0.04	-0.01	0.12	0.03
<i>Anapiculatisporites cronafferus</i>	0.26	-0.28	-0.04	-0.16
<i>Uvaesporites argenteaformis</i>	0.01	0.12	0.22	-0.07
<i>Nevesisporites bigranulatus</i>	-0.13	0.11	0.12	-0.12

TABLE 2. (cont.)

Principal component:	1	2	3	4
<i>Laevigatosporites couperi</i>	-0.16	-0.28	0.49	-0.21
<i>Lygodioisporites perverrucatus</i>	-0.07	0.04	0.03	-0.02
<i>Plicatella tricornitata</i>	-0.02	-0.27	-0.16	-0.17
<i>Reticulisporites venulosus</i>	-0.05	-0.13	-0.11	-0.05
<i>Cicatricosisporites dorogensis</i>	-0.15	-0.32	-0.42	-0.06
<i>Murospora</i> spp.	-0.03	-0.25	-0.11	-0.12
<i>Clavifera triplex</i>	0.17	-0.05	0.04	0.21
<i>Zebрасporites</i> spp.	0.52	-0.08	0.09	-0.11
<i>Classopollis torosus</i>	-0.11	0.24	0.20	-0.05
<i>Classopollis reclusus</i>	-0.12	-0.01	-0.35	-0.03
<i>Classopollis meyeriana</i>	0.47	0.21	0.04	-0.10
<i>Inaperturopollenites australis</i>	-0.37	0.12	0.29	-0.10
<i>Chasmatosporites</i> spp.	0.12	0.02	0.08	0.16
<i>Schizosporis spriggi</i>	-0.06	-0.25	-0.18	-0.10
<i>Peltandripites tener</i>	-0.03	-0.04	-0.09	-0.01
<i>Undulatasporites callosus</i>	-0.01	0.01	-0.03	0
<i>Naiaditaspora anglica</i>	0.27	-0.11	0.02	-0.13
<i>Cycadopites carpentieri</i>	-0.10	-0.03	0.08	0.08
<i>Cycadopites subgranulosus</i>	0.15	-0.05	0.04	0.21
<i>Cycadopites minimus</i>	0.15	-0.07	0.07	0.38
<i>Clavatipollenites hughesii</i>	-0.08	-0.09	-0.22	0.03
<i>Eucommiidites troedssonii</i>	-0.06	-0.20	-0.15	0.02
<i>Phyllocladites microreticulatus</i>	-0.05	-0.05	-0.03	-0.11
<i>Walchites</i> sp.	-0.12	0.11	0.14	-0.14
<i>Vitreisporites pallidus</i>	0.08	-0.19	-0.13	0.17
<i>Spheripollenites scabratus</i>	-0.08	-0.04	-0.06	0.21
<i>Spheripollenites psilatus</i>	-0.24	0.22	0.21	-0.23
<i>Pinuspollenites minimus</i>	-0.08	-0.18	-0.19	-0.09
<i>Alisporites dunrobinensis</i>	0.26	0.01	0.11	0.29
<i>Alisporites microsaccus</i>	0.11	0.46	0.24	-0.21
<i>Alisporites thomassii</i>	0.45	0.19	0.21	0.17
<i>Alisporites robustus</i>	-0.03	-0.13	0.16	0.40
<i>Pityosporites similis</i>	-0.30	-0.06	-0.35	-0.10
<i>Pityosporites microalatus</i>	-0.23	-0.01	-0.19	0.04
<i>Pityosporites scaurus</i>	0.04	-0.11	0.12	0.31
<i>Polonisaccus ferrugineus</i>	-0.02	0.03	0.09	0.03
<i>Parvisaccites enigmatus</i>	0.40	-0.12	0.12	-0.07
<i>Platysaccus papilionus</i>	0.52	0.03	0.08	-0.08
<i>Podocarpites reductus</i>	-0.18	0.13	0.29	-0.17
<i>Palaeoconifereus asecatius</i>	-0.02	0.01	0.03	0.04
<i>Callialasporites dampieri</i>	-0.34	0.24	0.23	-0.37
<i>Callialasporites turbatus</i>	-0.23	0.16	0.26	-0.18
<i>Callialasporites trilobatus</i>	-0.07	-0.04	0.04	-0.09
<i>Callialasporites microvelatus</i>	-0.25	0.25	0.28	-0.29
<i>Cerebropollenites macroverrucosus</i>	-0.24	-0.18	-0.12	-0.04
<i>Perinopollenites elatoides</i>	-0.35	0.18	0.23	-0.06
<i>Perinopollenites tumulosus</i>	-0.04	-0.15	-0.10	0
<i>Microcachrydites antarcticus</i>	-0.01	-0.02	0.01	0.04
<i>Clavatipollenites</i> - Rhaetic sp.	0.02	0.03	0.02	0.06
<i>Densoisporites</i> (Rhaetic spp.)	0.46	0	0.06	-0.14
<i>Taeniaesporites rhaeticus</i>	0.27	0.11	0.04	0.04
<i>Anemiidites echinatus</i>	0.54	-0.15	0.08	-0.08
<i>Granuloperculatipollis rudis</i>	0.09	0.13	0.01	-0.04

TABLE 2. (cont.)

Principal component:	1	2	3	4
<i>Limbosporites hundsbladii</i>	0.25	0.02	0.05	0.08
<i>Ovalipollis ovalis</i>	0.33	0.36	0.03	-0.10
<i>Rhaetipollis germanicus</i>	0.37	0.36	0.04	-0.09
<i>Cornutisporites seeburgensis</i>	0.17	-0.02	0.03	0.02
<i>Semiretisporis guthae</i>	0.15	-0.01	0.04	0.01
<i>Aratrisporites fimbriatus</i>	0.03	0.03	0.02	0.07
<i>Protohaploxypinus microcorpus</i>	0.07	0.02	0.03	0.08
Proportion of total variance (per cent.)	5.51	3.64	3.62	2.93

own opinion. *Vitreisporites pallidus* illustrates some of the problems: Couper (1958) thought it was from a caytonialean; Filatoff (1975) thought it was a cycad spore; while many subsequent palynologists have attributed it to a conifer.

INTERPRETATION OF THE POLLEN GROUPINGS

There are four reasons for our interpretations of the palynological groupings emerging from the statistical analyses.

One reason for our climatic interpretation is that, as the geographical and chronological spread of the evidence increases, the patterns revealed by multivariate statistical analyses rapidly become more general. In Quaternary studies, 'ecological' patterns give way to 'climatic' ones when the data from one geographical region are augmented by information scattered across a continent. When the chronological scale is extended to tens of millions of years from tens of thousands of years, in our experience temperature alone dominates as the source of variance in the statistical analyses based on correlation matrices. Oddly enough, evolution seems to contribute relatively little variance in these kinds of analyses, even with dinoflagellates whose fast reproduction and changing cyst-types imply rapid evolution, which would lead one to expect such problems. (Observer-errors in the form of taxonomic inconsistencies between microscopists can be an even more important source of variance. Changing patterns of catchment and transport of pollen can have dramatic effects on pollen spectra; thus the non-trivial principal components typically account for 90-95 per cent. of the total variance in a Pleistocene pollen analysis, while in deep boreholes and other deposits with complex taphonomies the figure falls to 60-70 per cent.) The dominant role of temperature in long-term climatic developments is illustrated in our Tertiary studies (Hubbard *et al.* 1994) where the pollen and dinoflagellate cyst records parallel the temperature record from oxygen isotope analyses in an unmistakable way.

Secondly, and more specifically, the Sun is the Earth's major heat source, and the Second Law of Thermodynamics ensures that warmth is distributed quite rapidly from the equatorial regions to both poles equally. The distribution of moisture is essentially a secondary process driven by this primary flow of insolation-derived heat. Le Chatelier's Principle similarly demands that concentrations of water vapour tend to equilibrate, but the process is slower and is strongly influenced by local factors, as the world's deserts show. Low humidity, however, tends to lead to low vegetational cover, and to low pollen production. There are therefore excellent *a priori* grounds for expecting correlations that are made over long distances (and particularly ones between the southern and northern hemispheres) to reflect temperature changes on a world-wide scale.

These considerations, with the uniformitarian principle that the (distant) past behaved in the same way as the relatively recent, and Occam's *entia non sunt multiplicanda praeter necessitatem*, led us to expect our results to be interpretable in terms of global temperatures. In fact, although they

lack subjective appeal, these arguments demand that no other interpretations should be considered unless temperature change can be excluded.

If these last two reasons insist that our findings must be interpreted in terms of global temperatures, the specific identifications of our climatic groupings are more ambiguous. Our initial assignment to our palynological groups of climatic associations arose from the recognition from the Australian evidence, that the groupings corresponded quite strongly to phylogenetic structures. Group S I is dominated by conifers, S II by primitive gymnosperms (e.g. Cheirolepidiaceae, cycads), and S III by moss- and fern-like organisms (a similar pattern is detectable in the northern hemisphere results, but is obscured by the complexity and far greater heterogeneity of the raw data). The correlation implied that Group S I was associated with much cooler and drier conditions than the others (since conifers are conspicuously more tolerant of drought and cold than ferns, mosses, and cycads) and that S III was tropical in character.

Further evidence for this general interpretation comes from the inverse correlation between the representation of our cold-climate group in the Hasty Bank section (Text-fig. 4) and the absolute concentrations of megafossils recorded by Hill (*in* Spicer and Hill 1979). At the base of the Hasty Bank section, the absolute concentration of macro-remains was about 80000 per m³. Immediately above this the concentration rose to around 130000 per m³, then it declined irregularly to about 10000 per m³. Other things being equal, this pattern suggests a climatically controlled increase and decrease in primary production, consistent with our climatic interpretations.

Given that group S II is strongly represented in the Australian strata the colour of which could suggest either arid or humid tropical conditions (Filatoff 1975) it is conceivable that the attributions of our tropical and intermediate groups might be inverted. Such a re-attribution would pose problems, however. Group N II dominates the Rhaetian pollen spectra at Kendelbach (Morbey 1975) (Text-fig. 7), and the aeolian character of many later Triassic terrestrial sediments has generally been taken to imply an arid climate, not a humid one.

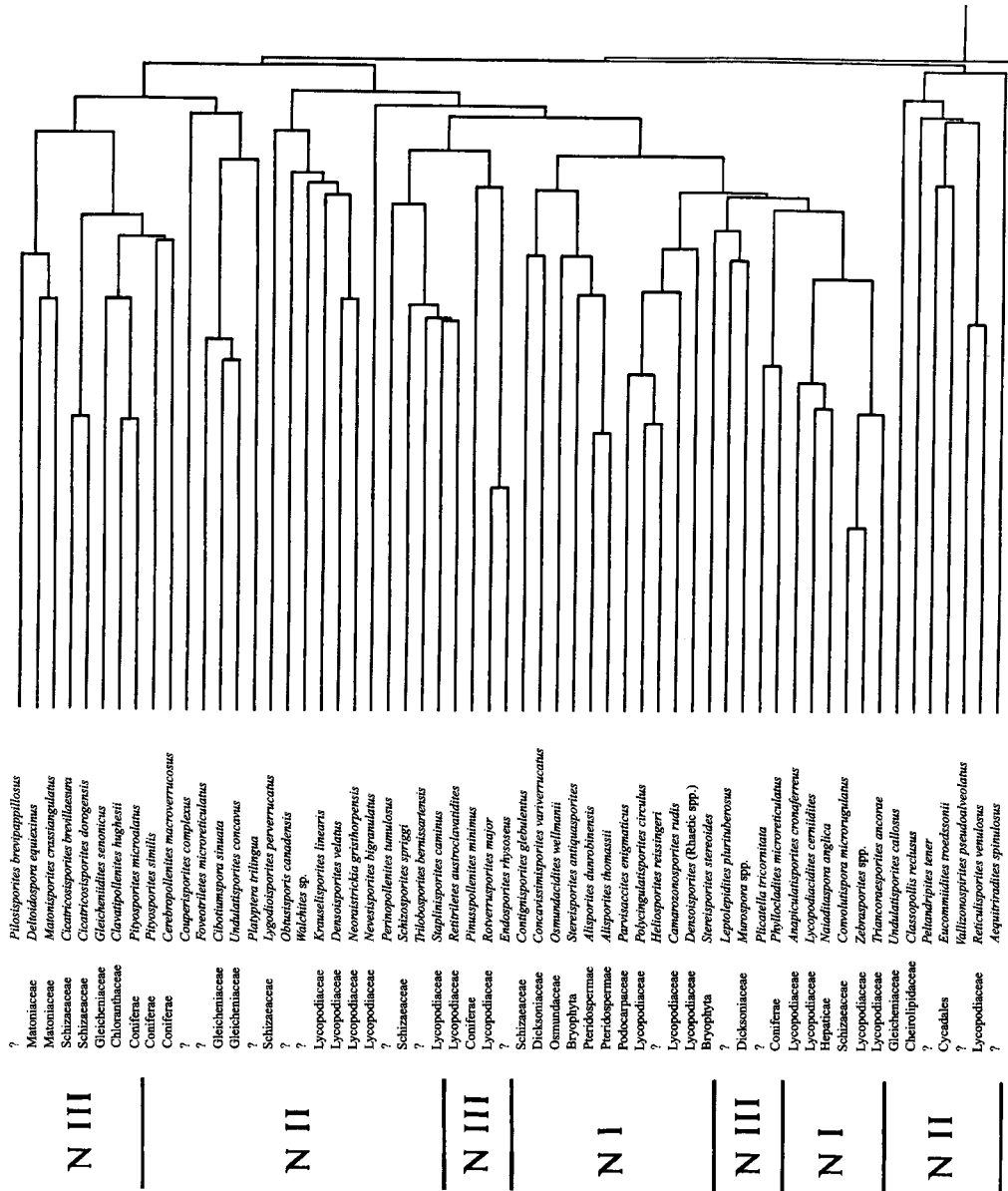
It is frustrating that both the northern and southern hemisphere sets of data come from rather similar latitudes, limiting the deductions that can be made on internal evidence. None the less, the climatic interpretations we have placed on our groupings can be seen to show both internal consistency, and consistency with their palaeogeographical contexts. Comparison of the climatic conditions associated with the 15 or so pollen and spore types which occur in both hemispheres reveals that about 40 per cent. belong to the equivalent climatic group (e.g. *Gleicheniidites senonicus*, *Vitreisporites pallidus*), and just under half move from N I to S II (e.g. *Calamospora mesozoica*, *Dictyophyllidites harrisii*), consistent with the differences in palaeolatitude. Only two (*Callialasporites turbatus*, *Matonisporites crassiangularatus*) shift in the 'wrong direction'.

Once the palynological groupings have been related to approximate climatic conditions, then these can be used to make crude climatic reconstructions (Hubbard and Boulter 1983) (see below); Text-figures 4 and 7 show estimates of summer and winter temperatures calculated in this way.

CORRELATION AND DATING

We have correlated one Yorkshire pollen sequence (Hasty Bank) spanning the Toarcian–Aalenian boundary with the Australian master sequence. Other British sequences correlated with the Australian diagrams identify the position of the Aalenian–Bajocian boundary; and a pair of Bathonian sequences are thought to span the *Morrisiceras morrisi* – *Proceras hodsoni* Opper-zone boundary (Text-fig. 4). Our correlations are consistent with the existing ammonite evidence, but (being based on quantitative analyses) are more accurate and reliable.

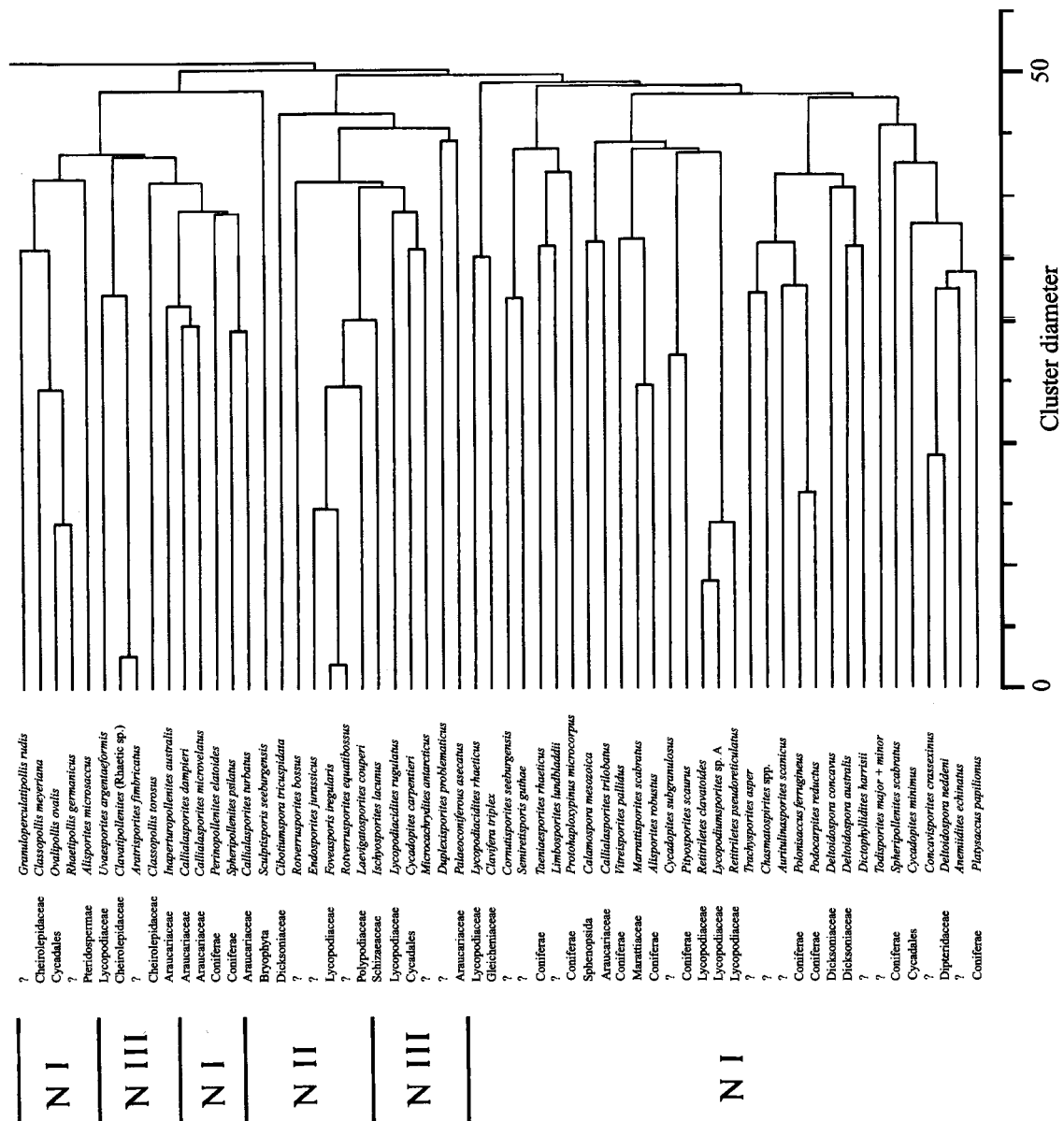
The absolute chronology of the Jurassic and Triassic periods has long been a matter of controversy. Our objectively based estimates of the relative lengths of the Aalenian, Bajocian and Bathonian stages show that the 'standard' chronology (Hallam *et al.* 1985) is much less satisfactory than van Hinte's chronologies (1976). Our most accurately defined points are in closer agreement with the latter's preferred chronology, which has therefore been used as the chronological basis of



TEXT-FIG. 3. For caption see opposite.

our work. Table 5 gives our key datings using the optimum fit between our relative chronology and van Hinte's.

Although the Bajocian–Bathonian boundary is not defined by any of the sequences studied, its position can be estimated with some accuracy. In the Aalenian and earlier Bajocian, the Opeel ammonite zones seem to correspond to warm-to-warm cycles (which would imply the extinction of cold-loving ammonites by warm episodes) whose periodicities averaged 1.42 million years (Ma) – indicating a date of about 162.7 Ma for the base of the Bathonian. With the *Morrisiceras morrisoni*–*Procerites hodsoni* boundary apparently fixed by the Gristhorpe and Cambridge sections, one can



TEXT-FIG. 3. Average Link dendrogram showing the relationships between the northern hemisphere Mesozoic pollen and spores in the 680 samples involved in this study. Sporomorphs of essentially cold environments are designated as Group N I, thermophilous ones are classified as Group N III; and Group N II contains the climatically intermediate taxa. The attributions of the palynomorphs to families are very speculative, but follow the opinions of the European palynologists cited.

calculate that in the Bathonian, the average duration of an Oppel-zone was rather shorter (0.80 Ma). Application of this estimate above the fixed Bathonian horizon supports Filatoff's idea that the sharp warming at about 155 Ma is indeed the Bathonian–Callovian boundary.

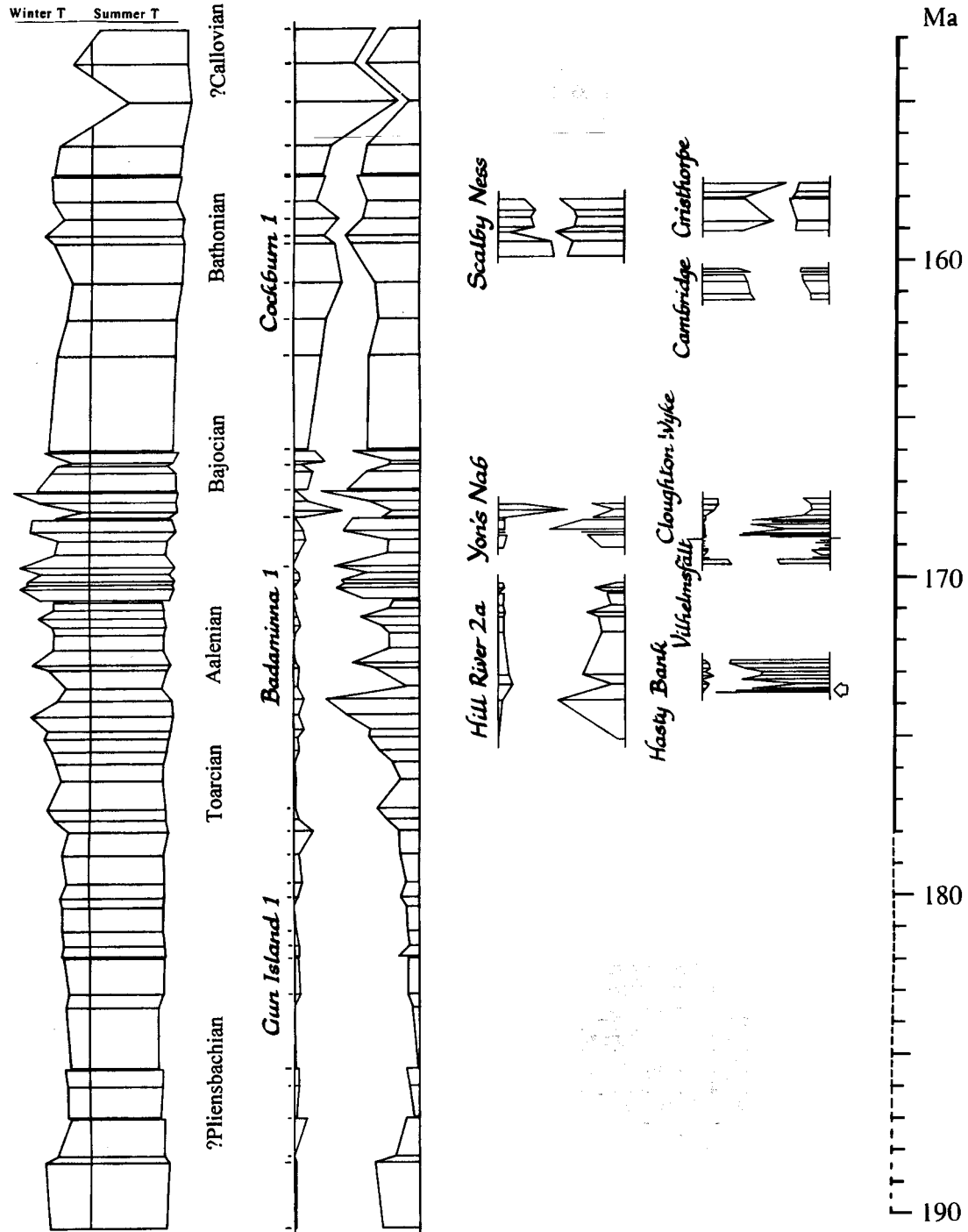
The accuracy with which correlations may be made using such quantitative evidence sometimes poses problems. The precision of the correlation depends – other things being equal – on the

TABLE 3. Simplified enumeration of the rotated principal components yielded by the Australian data. The values tabulated are rounded integer tenfold multiples of the rotated principal component loadings (thus a value of 7 reflects a loading between +0.65 and 0.74): loadings of less than 0.25 (regardless of sign) have been ignored.

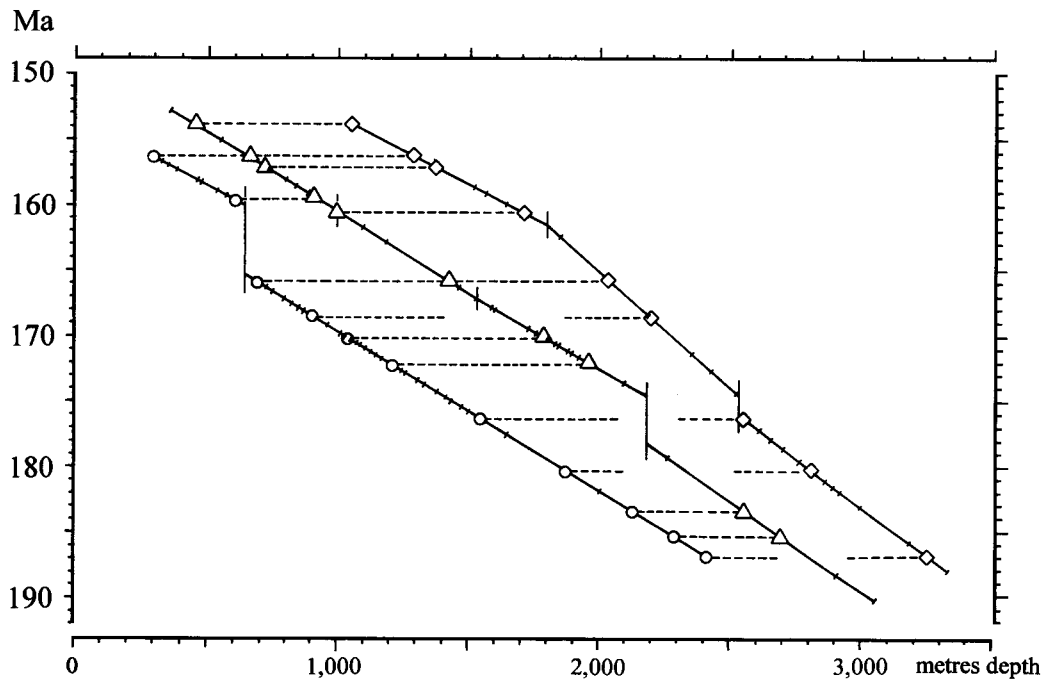
Rotated principal component:	1	2	3	4	5	6	7	8	9	10	11	12	13	14	15	16	17	18	19	20
<i>Stereisporites psilatus</i>
<i>Stereisporites antiquasporites</i>	.	.	7
<i>Rogalskiasporites cicatricosus</i>	8
<i>Rogalskiasporites canaliculus</i>	5	.	5
<i>Polycingulatisporites crenulatus</i>	6	3
<i>Polycingulatisporites striatus</i>
<i>Antulsporites varigranulatus</i>	3	6
<i>Antulsporites clavus</i>	8
<i>Antulsporites saevus</i>	8
<i>Foveosporites moretonensis</i>	5	3
<i>Staplinsporites caminus</i>	5	5	.
<i>Staplinsporites telatus</i>	.	.	3	.	7	3
<i>Staplinsporites mathurii</i>
<i>Staplinsporites perforatus</i>	.	.	6
<i>Foveosporites multifoveolatus</i>	8
<i>Foveotriletes cf. irregulatus</i>
<i>Densoisporites circumundulatus</i>	7
<i>Densoisporites sp. A</i>
<i>Densoisporites sp. B</i>
<i>Lycopodiacidites cerniidites</i>
<i>Camazonosporites ramosus</i>	8	.	3
<i>Camazonosporites clivus</i>	4	.	5	.	.	6
<i>Leptolepidites major</i>	7
<i>Uvaesporites equibossus</i>	4	3
<i>Uvaesporites crassibalteus</i>	3
<i>Uvaesporites sp.</i>
<i>Lophotriletes sp.</i>	7
<i>Apiculatosporites</i>	7
<i>Acanthotriletes levindensis</i>	.	8
<i>Conbaculatisporites cf. mesozoicus</i>	.	.	.	9
<i>Neoraistrickia taylorii</i>	8
<i>Neoraistrickia pilobaculata</i>	3	.	3	.	.	5
<i>Neoraistrickia trichosa</i>	.	9
<i>Neoraistrickia densata</i>	4	.	7	3
<i>Neoraistrickia truncata</i>	.	.	4	.	3	.	.	6
<i>Neoraistrickia sp. A</i>	.	.	.	9
<i>Neoraistrickia spp.</i>	.	7
<i>Lycopodiumsporites rosewoodensis</i>
<i>Lycopodiumsporites reticulumsporites</i>	3	7
<i>Lycopodiumsporites austroclavatis</i>	.	4	3	.	-4	.	3
<i>Lycopodiumsporites circolumensis</i>	.	.	5	.	.	6
<i>Lycopodiumsporites sp. A</i>
<i>Lycopodiumsporites spp.</i>	6	3
<i>Dictyosporites speciosus</i>	8
<i>Dictyosporites complex</i>	.	9
<i>Paxillitriletes</i>
<i>Pilasporites marcidus</i>	4
<i>Calamospora mesozoica</i>	8	.
<i>Marattisporites scabratus</i>	3
<i>Todisporites minor</i>
<i>Osmundacidites wellmanii</i>	.	.	.	5	3
<i>Baculatisporites comaumensis</i>	6
<i>Verrucosisporites varians</i>
<i>Verrucosisporites rugulodomus</i>
<i>Rugulatisporites chamiomatus</i>	3	.	.	.

21	22	23	24	25	26	27	28	29	30	31	32	33	34	35	36	37	38	39	40
													7						
						7													
							3												
						3													
		4																	
													5						
						3													
																	8		
											8								
		7																	
				7															
				3															
				3			5								-3				
																			9
										3					3				4
											8								
		7																	
8										7				6					
			4																
				3						4									
					3		7												
7														7					

21	22	23	24	25	26	27	28	29	30	31	32	33	34	35	36	37	38	39	40
.	3
.	3
.	7	3
.	3
.
.
.	8	3	3
.
.	.	9
.	.	5
.	.	.	-3	-3
.	.	.	.	5
5	.	.	.	3	7
.	7
.	8	.	.	.
.
.	3	.	.
.	7
.
.	4
.	8
.	3
.	3
.	-4
.
.
.
.
3	3	5
.
.
.
.
.	3
.	8	.	.
8
7
.	5	3



TEXT-FIG. 4. Australian and European earlier Jurassic pollen diagrams. The left-hand part of the figure shows composite plots of climatic reconstructions (winter and summer temperatures) and pollen diagrams for the earlier Jurassic in Western Australia. The left-hand hatched areas in the pollen diagrams are the warmth-loving species (S III), the right-hand hatched areas the types indicative of cool climates (S I), and the blank areas

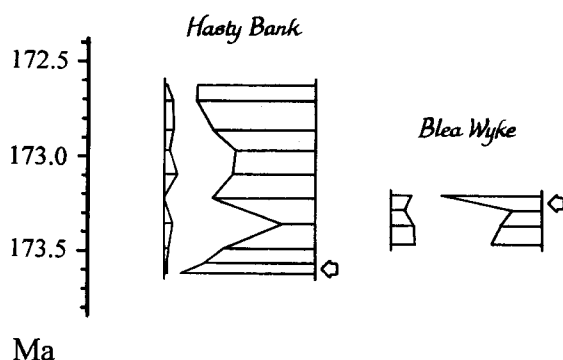


TEXT-FIG. 5. Age-versus-depth plots for the Cockburn 1, Badaminna 1 and Gun Island 1 boreholes, showing the correlative points that provide the justification for the confluents in Text-fig. 4. The crucial points in the Badaminna 1 borehole are indicated with circles, those at Cockburn 1 with triangles, those at Gun Island 1 with diamonds. Other sample points are shown by cross bars.

TABLE 5. Selected chronological events identified in the pollen diagrams, the dates of which can therefore be related to our modified version of van Hinte's chronology (1976).

Stratigraphical event	Time
<i>Morrisceras morrissi</i> - <i>Procerites hodsoni</i> boundary (Lower-Middle Bathonian boundary)	158.62 Ma
Bathonian-Bajocian boundary	162.7 Ma
? <i>Stephanodiscus humphriesianum</i> - <i>Emileia</i> (<i>Otoites</i>) <i>sauzei</i> boundary	165.89 Ma
Millepore Bed	168.68 Ma
Bajocian-Aalenian boundary	170.15 Ma
Eller Beck Bed	170.5 Ma
Aalenian-Toarcian boundary	173.5 Ma

between depict the climatically intermediate taxa (S II). At the right hand side of the figure, some of the correlative pollen diagrams from north-west Europe and Australia are shown. The vertical scale is in millions of years, using the chronology of van Hinte (1976). The Toarcian-Aalenian boundary is arrowed. (The elements of the composite Australian pollen diagram are identified by marginal marks. Spectra from the Cockburn 1 borehole are indicated by long bars, those from Gun Island 1 by short bars, and the Badaminna spectra are unmarked.)



TEXT-FIG. 6. Toarcian–Aalenian pollen diagrams from Yorkshire, showing the various positions at which the boundary (arrowed) has been placed by Muir (1964) at Hasty Bank and Wilkinson (1978) at Blea Wyke. Conventions as for Text-fig. 4.

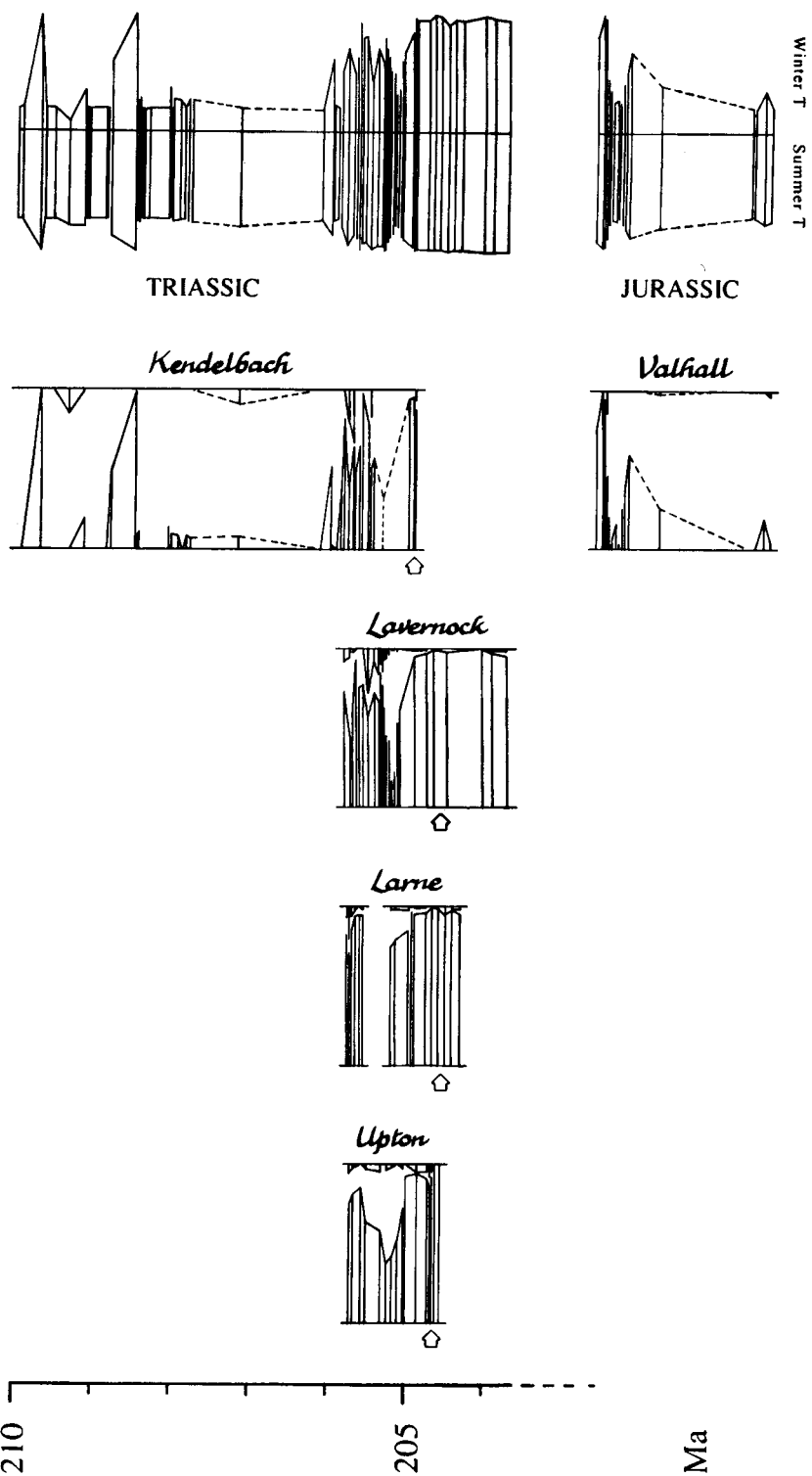
stratigraphical resolution of the curves being matched. The more detailed sections of the Australian master-sequence clearly have a resolution of a few hundreds of thousands of years, and some of the European profiles are sampled at intervals of less than a hundred thousand years. Since it is the patterns that are being matched and not individual spectra, the precision is rather greater than either of these figures suggests. At this level of accuracy, inconsistencies in the positions of the stage boundaries can be perceptible. For instance, the Toarcian–Aalenian boundary was placed by Muir (1964) in the warming period preceding the warm episode, at about 173.59 Ma. However, Couper's (1958) Whitby sequence and Wilkinson's (1978) analyses of Blea Wyke Point seem to place the boundary about 350 000 years later, at the end of the warm oscillation (Text-fig. 6). Clearly an examination is needed of the definition of the Toarcian–Aalenian boundary and how it relates to these sequences. Other sequences are too closely sampled to be correlatable at present; for instance, the 13 samples analysed by Muir from the 0.9 m Low Beast Cliff section record a sharp N III peak followed by an equally sharp minimum in the N I group. Whether these warm episodes are 20 000, 40 000, or 100 000 years apart it is impossible to say, as the pattern cannot be matched in any of the closely sampled European Aalenian sequences, and the resolution of the Australian sequences is far too coarse.

THE TRIASSIC–JURASSIC BOUNDARY

Text-figure 7 shows the ecological and climatic developments in north central Pangaea in the final stage of the Triassic Period and at the boundary with the Jurassic. Given the absence of any convincing overlap between the sequences used in Text-figure 4 and these Rhaetian–Hettangian ones, the standard chronology (Forster and Warrington 1985) has been used. It was assumed that the Kendelbach deposits (Morbey 1975) spanned the entire Rhaetian stage.

The most important feature is the extremely dramatic cooling episode immediately below the Triassic–Jurassic boundary. It appears to have been considerably more intense (if slightly more gradual) than the global cooling that occurred just above the Eocene–Oligocene boundary (Shackleton 1986; Hubbard *et al.* 1994), when a global temperature drop of 6 °C took place. Although traditional ideas about global extinctions and climatic changes at the Triassic–Jurassic boundary have been questioned (Weems 1992), the graphs in Text-figure 7 provide direct evidence of major ecological crisis at this time – whether or not this caused mass extinctions.

Our evidence indicates that the earliest Jurassic marked a change to persistently and consistently colder conditions. Comparable climatic reconstructions in the Tertiary are demonstrably inaccurate for absolute values of temperature, but give realistic pictures of relative changes (Hubbard and Boulter 1983). In the circumstances, we have made no attempt to relate our climatic curve to exact temperatures. None the less it is fair to observe that, while the Aalenian–Bajocian cold episodes nominally reflect occasional mild winter frosts, the conditions indicated at the Triassic–Jurassic boundary are of consistently severe conditions for several hundred thousand years. It is not clear



TEXT-FIG. 7. Rhaetian-Hettangian pollen diagrams from northern Europe, showing the position of the Triassic-Jurassic boundary (arrowed) above the apex of a cold-temperature event. Conventions as for Text-fig. 4.

why the cooling process should have been slow and steady in comparison with the onset of the Early Oligocene event, let alone the Pleistocene glaciations. The Late Triassic cooling seems to have been preceded by an extended warm but probably arid period analogous to the one recorded in the bottom part (Sinemurian–Pliensbachian) of the Australian Jurassic sequences.

The pollen diagrams from Valhall in Scania (Guy-Ohlson 1981) and Rodby in Denmark (Lund 1977) were from strata the age of which was thought to be close to the beginning of the Hettangian or (in the case of Rodby) spanning the Triassic–Jurassic boundary. In neither case can the very characteristic ‘vegetational fingerprint’ of the Rhaetian–Hettangian boundary be recognized. In both cases, the pollen diagrams show intermittent sharp cold oscillations that become less and less severe. In both cases, the overall structure of the vegetation is unmistakably Jurassic and not Triassic in character when assessed by our methods. We therefore conclude that the deposits sampled are probably not older than the middle Hettangian.

CLIMATIC IMPLICATIONS

Our studies put traditional views of middle Mesozoic climates in a fresh perspective. The Late Triassic and earlier Jurassic seem to have had a broadly similar climate – torrid and apparently fairly stable – with the ‘cold event’ at the Jurassic boundary breaking the continuity and possibly causing mass extinctions. This frigid episode seems to have been preceded by one major cold oscillation, with which the Vallis Vale sequence (Orbell 1972) can be correlated. Several short cold fluctuations of decreasing severity followed later in the Hettangian, which are recorded in the Valhall borehole, and apparently at Rodby in Denmark. There is some evidence for a distinct shift to warmer conditions between the Rhaetian and the Hettangian periods: two pollen types classified as tropical in purely Triassic contexts (*Perinopollenites elatoides*, *Inaperturopollenites australis*) are intermediate (Group N II) in Jurassic contexts. This also serves to remind us that if the intermediate groups are associated with aridity, not all of the taxa within these gross agglomerations are necessarily of that character.

The Toarcian seems to have heralded the onset of a Middle Jurassic climatic regime with rather regular but not extreme climatic oscillations, and perhaps increasing humidity. Overall temperatures dropped slightly to a nadir near the Aalenian–Bajocian boundary, and then increased gradually to the Bathonian–Callovian boundary. The middle and upper Bathonian seem to have reverted to a rather cooler climate. The Callovian climate appears to have been warm and humid.

In later Jurassic and earliest Cretaceous times the contribution of plants associated with warm and arid conditions is greatly reduced, and small-scale climatic oscillations were constantly taking place as in the earlier Pleistocene. The climate seems to have been similar to that of the Callovian. The rather fundamental changes that took place some time between 140 and 150 Ma may be connected with the emergence of the proto-Atlantic Ocean. If the two phenomena are indeed related, then they supply yet another example (with the Tertiary thermal maximum, the formation of the Antarctic ice cap in the Oligocene, and the Pleistocene glaciations) of the profound influence of continental and ocean basin geometry on global climate.

CONCLUSIONS

Our results demonstrate that quantitative palynology can be used, in favourable circumstances, for precise and unambiguous correlations in the Jurassic as in the Quaternary. The key to this is a knowledge of the ecological and climatic preferences of the plants involved, and this in turn can be deduced from the internal evidence of quantitative palynological analyses. Multivariate statistical methods – in particular principal components analysis – are the most effective way currently available of identifying the requisite patterns in the data. The climatic patterns emerging from the palynological evidence provide ample grounds for the traditional idea of mass extinctions at the Triassic–Jurassic boundary.

Acknowledgements. We are grateful to an anonymous referee who pointed out blemishes in a much earlier version of this article, and to Dr F. H. Jardine for his refinements of the text. Dr J. T. Parrish pointed out a number of inconsistencies and inaccuracies that had crept into the revised text. Dr Mary Dettmann made some valuable suggestions, and spotted a further crop of corrigenda. Dr C. R. Hill gave much valuable advice at an early stage in this research.

REFERENCES

- BIRKS, H. J. B. and BIRKS, H. H. 1980. *Quaternary palaeoecology*. E. Arnold, London, viii + 289 pp.
- BOULTER, M. C. and WINDLE, T. 1993. A reconstruction of some Middle Jurassic vegetation in northern Europe. *Special Papers in Palaeontology*, **49**, 125–154.
- COUPER, R. A. 1958. British Mesozoic microspores and pollen grains. *Palaeontographica, Abteilung B*, **103**, 75–179.
- FILATOFF, J. 1975. Jurassic palynology of the Perth Basin, Western Australia. *Palaeontographica, Abteilung B*, **154**, 1–113.
- FORSTER, S. C. and WARRINGTON, G. 1985. Geochronology of the Carboniferous, Permian and Triassic. *Memoirs of the Geological Society, London*, **10**, 99–113.
- GUY, D. J. E. 1971. Palynological investigations in the Middle Jurassic of the Vilhelmsfält boring, southern Sweden. *Publications from the Institutes of Mineralogy, Palaeontology, and Quaternary Geology, University of Lund*, **168**, 1–104.
- GUY-OHLSON, D. J. E. 1981. Rhaeto-Liassic palynostratigraphy of the Valhall bore No. 1, Scania. *Geologiska Föreningens i Stockholms Förhandlingar*, **103**, 233–248.
- 1982. Biostratigraphy of the Lower Jurassic–Cretaceous unconformity at Kullemölla, southern Sweden. *Sveriges Geologiska Undersökning, Rapporter och Meddelanden*, **52**, 1–45.
- 1990. Pliensbachian palynology of the Karindal bore no. 1, north-west Scania, Sweden. *Review of Palaeobotany and Palynology*, **65**, 217–228.
- HALLAM, A., HANCOCK, J. M., BRECQUE, J. L. La, LAWRIE, W. and CHANNELL, J. E. T. 1985. Jurassic to Palaeogene: Part 1 Jurassic and Cretaceous geochronology, and Jurassic to Palaeogene magnetostratigraphy. *Memoirs of the Geological Society, London*, **10**, 118–140.
- HINTE, J. E. van 1976. A Jurassic time scale. *Bulletin of the American Association of Petroleum Geologists*, **60**, 489–497.
- HUBBARD, R. N. L. B. and BOULTER, M. C. 1983. Reconstruction of Palaeogene climate from palynological evidence. *Nature*, **301**, 147–150.
- BOULTER, M. C. and MANUM, S. B. 1994. Cenozoic dinoflagellate palaeoecology elucidated, and used for marine-terrestrial biological correlation. 57–72. In BOULTER, M. C. and FISHER, H. C. (eds). *Cenozoic plants and climates of the Arctic*. NATO A.S.I. Series I, 27. Springer Verlag, Berlin, viii + 401 pp.
- IMBRIE, J. and KIPP, N. G. 1971. A new micropaleontological method for quantitative paleontology. 71–182. In TUREKIAN, K. K. (ed). *The Late Cenozoic glacial ages*. Yale University Press. New Haven, xii + 606 pp.
- LUND, J. J. 1977. Rhaetic to Lower Liassic palynology of the onshore south-eastern North Sea Basin. *Danmarks Geologiske Undersøgelse II Rk.*, **109**, 1–129.
- MORBAY, S. J. 1975. The palynostratigraphy of the Rhaetian Stage, Upper Triassic in the Kendelbach graben. *Palaeontographica, Abteilung B*, **152**, 1–75.
- MUIR, M. D. 1964. The palaeoecology of the small spores of the Middle Jurassic of Yorkshire. Unpublished Ph.D. thesis, University of London.
- NORRIS, G. 1963. Upper Jurassic and Lower Cretaceous microspores and microplankton from southern England. Unpublished Ph.D. thesis, University of Cambridge.
- ORBELL, G. 1972. The palynology of the Triassic–Jurassic transition in Britain. Unpublished Ph.D. thesis, University of London.
- 1973. Palynology of the British Rhaeto-Liassic. *Bulletin of the Geological Survey of Great Britain*, **44**, 1–44.
- RIDING, J. B. 1983. The palynology of the Aalenian (Middle Jurassic) sediments of Jackdaw Quarry, Gloucestershire, England. *Mercian Geologist*, **9**, 111–120.
- SHACKLETON, N. J. 1986. Paleogene stable isotope events. *Palaeogeography, Palaeoclimatology, Palaeoecology*, **57**, 91–102.
- SPIKER, R. A. and HILL, C. R. 1979. Principal Components and Correspondence Analyses of quantitative data from a Jurassic plant bed. *Review of Palaeobotany and Palynology*, **28**, 273–299.

- WEEMS, R. E. 1992. The "terminal Triassic catastrophic extinction event" in perspective: a review of Carboniferous through Early Jurassic terrestrial vertebrate extinction patterns. *Palaeogeography, Palaeoclimatology, Palaeoecology*, **94**, 1–29.
- WILKINSON, G. C. 1978. Jurassic palynology from a North Sea core. Unpublished M.Sc. thesis, University of Sheffield.

R. N. L. B. HUBBARD

M. C. BOULTER

Palaeobiology Research Unit
University of East London
London E15 4LZ, UK

Typescript received 22 June 1995

Revised typescript received 19 January 1996